# Optical-absorption spectrum of polyacetylene: Effect of lattice deformation, impurities, and end conditions

Arnold J. Glick
*Department of Physics and Astronomy, University of Maryland, College Park, Maryland 20742*

Garnett W. Bryant
*McDonnell Douglas Research Laboratories, St. Louis, Missouri 63166*
(Received 22 October 1984; revised manuscript received 31 January 1986)

The optical-absorption spectrum and other properties of *trans*-polyacetylene chains are calculated for different lattice configurations: dimerized, soliton, and polaron, with and without impurities, for chains with an even or an odd number of lattice sites. The effect of different end conditions is investigated. The absence of free solitons in pure polyacetylene is explained. Bound solitons provide the most favorable configuration when the system is doped; however, we also show how doping can generate free solitons when the impurities are associated with the ends of chains. Comparison of the results with experimental spectra gives information about the microstructure of real films.

## I. INTRODUCTION

Measurements[1-4] of the optical-absorption spectra of pure and doped *trans*-polyacetylene, $(CH)_x$, have been used to support the theory[5-7] that solitons (kinks) form in the $(CH)_x$ lattice when it is doped. Solitons are associated with a state in the middle of the energy gap between the $\pi$-electron valence and conduction bands. The absorption spectrum displays structure for doped samples which onsets near the middle of the region below the interband threshold. As doping concentration increases, this below-interband (BI) absorption grows with a concomitant decrease in interband absorption. This structure has been attributed to the presence of solitons. However, further investigation is needed to improve the theoretical description of the chains as well as to clarify the connection between the microscopic structure and the measured spectrum. The measured BI absorption is broader than that predicted by the simple soliton theory,[8-10] and the simple theory neglects the influence of the impurity potential on the soliton state. Also, other defect structures besides solitons (e.g., polarons) can exist on the chains and affect the spectrum.

We have studied[11] the spectra associated with a variety of chain-impurity configurations. We also considered finite-chain effects, namely, the dependence on lattice length (odd-even effect) and on end conditions. The results we obtained show clearly how energy considerations eliminate certain configurations, while others are likely to occur. The observed spectrum is expected to be a composite arising from samples containing different allowed configurations. Here we present results for the energetically favored cases, and discuss the evidence that they actually occur in real films.

For a chain with an even number of carbon sites in the presence of an impurity, the chain will have a pure-dimerized structure if the chain is neutral and a polaron structure if the chain is charged. We show how the polaron configuration is modified by the presence of the impurity. When the chain has an odd number of carbon sites, a soliton will be present. We consider how the soliton configuration is altered by the presence of the impurity and show the effect on the optical-absorption spectrum. Bound solitons provide the most stable configuration when the system is doped; however, the observed spectrum is more characteristic of free solitons. Our results for an impurity at the end of a chain shows that there is a mechanism for generating free solitons during the doping process. This latter process may provide the key needed to explain the experimental results.

In Sec. II, we describe our microscopic calculations. In Sec. III we report results for finite chains of sufficient length ($\sim$200 sites) so as to clearly distinguish end and bulk effects. The results for each case are represented by a plot of the absorption spectrum labeled by the associated ground-state energy and Fermi energy of the lattice, and plots of charge distribution along the chain. The charge distribution, aside from its intrinsic interest, can be used to more readily identify the case being represented as to location of solitons, and/or impurity, and end conditions. The ground-state energies can be used to compare the relative stability of different configurations.

Section IV contains a discussion of the implications of the results and questions raised by this investigation.

## II. MICROSCOPIC CALCULATIONS

We use the discrete lattice model of Su, Schrieffer, and Heeger[6,7] (SSH) to describe the $\pi$-electron system of $(CH)_x$. The details of this model and our application of it has been discussed elsewhere.[12,13] In the presence of an impurity there is an additional contribution to the Hamiltonian

$$U_{\rm imp}=\sum_{n,s} U_n C^{\dagger}_{n,s} C_{n,s} - \sum_n U_n \ , \tag{1}$$

where $C^{\dagger}_{n,s}$ creates a $\pi$ electron with spin $s$ at the $n$th CH group. The second term on the right is the interaction be-

 

tween the impurity and the charged $(CH)^+$ molecules. The dopant is modeled by a point charge that is located off the chain by a distance $d$ and is screened by the bulk dielectric constant[7] ($\epsilon=10$). The potential at the $n$th site is

$$U_n=\frac{-e^2}{\epsilon\,|\,(x_n-x_{\rm imp})^2+d^2\,|^{1/2}}\ , \tag{2}$$

where

$$x_n=na-u_n \tag{3}$$

is the position of the $n$th CH group including $u_n$, the displacement from its position on a uniform lattice. The impurity is adjacent to position $x_{\rm imp}$ on the chain. The value of $a$ is taken from observation and implicitly accounts for the correction to the lattice constant of the uniform chain due to harmonic coupling.[14]

We are dealing with chains of finite length, and the end conditions have an important effect on the results. Su[14] and Vanderbilt and Mele[15] have shown that it is energetically favorable for the dimerization pattern of the lattice to "relax" near the ends and to terminate with strong bonds. Similar relaxation can be seen in the self-consistent solutions of Stafström and Chao.[16] To simulate the relaxation we use the function suggested by Su, which at end $N$ takes the form

$$u_n=(-1)^n u_0\left[1+A\ \mathrm{sech}\left[\frac{N-n}{\xi}\right]\right]\ . \tag{4}$$

We find the optimum parameters to be $\xi=1$ and $A=0.54$ for an end without impurity and $A=0.52$ if there is an impurity near the end. This form represents an enhancement of the dimerization near the chain ends, i.e., an increase in the difference in bonding between alternate sites. The ground-state energy of the 200-site chain is lowered by 0.032 eV by this modification compared to the abrupt termination with a strong bond. Termination with a weak bond expends 1.07 eV and is not expected to occur.

As in Ref. 13, we diagonalize the Hamiltonian matrix to obtain the one-electron energies. However, here we also need the eigenfunctions for use in determining other properties of the system. Most of the calculations were performed for chains with either 199 or 200 CH groups and either no impurity or one impurity (a concentration of 0.5 percent impurities) adjacent to the chain. The latter corresponds to the lightly doped regime that has been studied extensively.[1-4,8] A Kubo-type calculation[17] gives the conductivity in terms of a density-current correlation function. Evaluating this function gives the real and imaginary parts of the site-averaged conductivity in the form

$$\mathrm{Re}\overline{\sigma(\omega)}=\sum_l\sum_m\frac{\overline{B_{lm}}\eta}{(\omega+\varepsilon_l-\varepsilon_m)^2+\eta^2}\ , \tag{5a}$$

$$\mathrm{Im}\overline{\sigma(\omega)}=\sum_l\sum_m\frac{\overline{B_{lm}}(\omega+\varepsilon_l-\varepsilon_m)}{(\omega+\varepsilon_l-\varepsilon_m)^2+\eta^2}\ . \tag{5b}$$

The sums are over single-particle states of energy $\varepsilon_l$ and $\varepsilon_m$ and

$$\overline{B_{lm}}=\frac{1}{N}\frac{e^2a}{\hbar^2}(\varepsilon_m-\varepsilon_l)\left|\sum_{j=1}^{N}x_j\psi_l(j)\psi_m^*(j)\right|^2\times\left[\frac{1}{e^{\beta\hbar(\varepsilon_l-\mu)}+1}-\frac{1}{e^{\beta\hbar(\varepsilon_m-\mu)}+1}\right]\ , \tag{6}$$

where $\psi_l(i)$ is the amplitude of the $l$th state on the $i$th site, and $\mu$ is the $\pi$-electron chemical potential.

For the calculations we report below, $\eta$ was kept finite. $\eta$ can be thought of as a lifetime due to neglected higher-order effects, or just as a smoothing parameter to account for the fact that a typical sample will contain chains of varying length. We used $\eta=0.1$ eV which is larger than the maximum level separation deep within the valence or conduction band of a 200-site chain. This value is sufficiently large to smooth most features which are expected to be smooth in an infinitely long chain. For shorter chains a larger value for $\eta$ is more appropriate. The effect of $\eta$ on the results is discussed in Sec. III.

Once the conductivity of a single chain is known, one can find the dynamic dielectric constant of a film

$$\epsilon(\omega)=\epsilon_0+4\pi i\rho_c\sigma(\omega)/\omega\ , \tag{7}$$

where $\rho_c$ is the density of chains per unit cross-sectional area. We assume $\rho_c=7\times10^{14}$ cm$^{-2}$, corresponding to a lattice of $(CH)_x$ chains each separated by about 4 Å. Equation (7) would be modified if it were necessary to account for a Lorentz correction.[18] However, the results we report below are not improved by such a correction.

The absorption coefficient for decay of an electromagnetic wave passing through the medium is given by twice the imaginary part of the propagation vector

$$2K=\sqrt{2}(\omega/c)[\,|\,\epsilon(\omega)\,|-\epsilon_1(\omega)]^{1/2}\ . \tag{8}$$

In this expression $\epsilon_1(\omega)$ is the real part of the dielectric constant.

The ground-state energy of the chain includes the lattice-distortion energy and the interaction of the singly charged lattice ions with the impurity potential. The energy is measured from $E_0(N)$, the ground-state energy of a uniform lattice (no dimerization) with the same number of particles.

In our calculations the lattice was not treated dynamically. Its form was fixed for each case considered. Consequently, the conductivity we present is valid in the optical range, but is not applicable to the infrared for which lattice vibrations play a crucial role. The low-frequency behavior is thus analogous to what would be found by employing the Drude theory.

The parameters used for the calculations are the same as were used in Ref. 13, namely:

$$t_0=2.5\ \text{eV},\quad u_0=0.042\ \text{Å}\ ,$$

$$K=21.0\ \text{eV/Å},\quad a=1.22\ \text{Å}\ ,$$

$$\alpha=4.16\ \text{eV/Å},\quad \beta=1000\ \text{eV}^{-1}\ .$$

## III. RESULTS

For a uniformly dimerized lattice with an even number of CH groups the basic molecular configuration is given by $u_n=(-1)^n u_0$. If the chain is neutral and in its ground state, the $\pi$ electrons occupy and fill the spin-degenerate valence band. Charge is distributed uniformly along the chain, and the optical-absorption spectrum presents only an interband peak. If an impurity is placed near the chain, an impurity level is pulled into the gap between the valence and conduction bands and the other states are also altered. If the chain remains neutral then the charge distribution of the $\pi$ electrons exhibits strong polarization fluctuations around the impurity site. This behavior is shown in the inset of Fig. 1 for a 200-site chain with an impurity $d=2$ Å away from the chain and adjacent to site 61. However, the impurity has little effect on the optical-absorption spectrum. There is no BI absorption. Absorption due to transitions from the valence band into the impurity level, which might be expected to onset at $\hbar\omega=1.2$ eV is not found. It is absent because of almost zero overlap of the wave functions near the top of the valence band and of the impurity state. The oscillations in the interband absorption, seen in Fig. 1, are also not expected to be observable in a real sample where they would be averaged over contributions from chains of a different length and impurity proximity to the chain.

When a chain with an even number of sites becomes charged by picking up or giving up an electron, the lattice develops a distortion around which the excess charge remains localized. This distortion is called a polaron, and it has the property that the phase of dimerization is the same on both sides of the disturbance. The possibility of polarons occurring on an SSH chain was suggested by Brazovskii and Kirova[19] and Campbell and Bishop.[20] Using the continuum form of the SSH model, they found that polarons are favored as the analytic solution when a trans-$(CH)_x$ chain is charged $Q=\pm 1$. Our calculations were performed using the discrete model with the same form for the polaron that we used earlier:[13]

$$u_n=-(-1)^n u_0\left[1-A_p\exp\left[-\frac{(n-p)^2}{l_p^2}\right]\right], \tag{9}$$

for a polaron centered at site $p$, with half-width spreading over $l_p$ sites. $A_p$ gives the maximum reduction in dimerization. Other forms for this distortion which have been reported in the literature give similar results for the energy of the polaron states.[21] We consider two cases: a chain with a polaron and no impurity and a chain with impurity and a polaron bound to the impurity. In both cases, we use the optimum values found in Ref. 12 for parameters $A_p$ and $l_p$.

The free polaron has width $l_p=12$ and $A_p=0.6$. With the polaron lattice distortion there are two electron gap states with energies $\pm 0.48$ eV. Figure 2 shows the results for a chain with $N=200$ and no impurity. The optical-absorption spectrum shows two peaks below the interband threshold. The higher energy peak arises from transitions between gap states. When the chain is charged positive (negative) the low-energy peak is due to transitions between the valence (conduction) band and the closest gap state.

When an impurity is present, the energy is optimized by using $l_p=8$ and $A_p=0.8$. Figure 3 shows the corresponding spectra and charge distribution. The peaks in the spectra associated with the gap states are closer to the middle of the BI region, but are still not consistent with the experimental spectra. Refer to Fig. 4 of Feldblum *et al.*[3] to see observed optical-absorption spectra of *trans*-$(CH)_x$ with different amounts of doping. Experiment shows a peak in the middle of the BI region ($\sim 0.7$ eV),

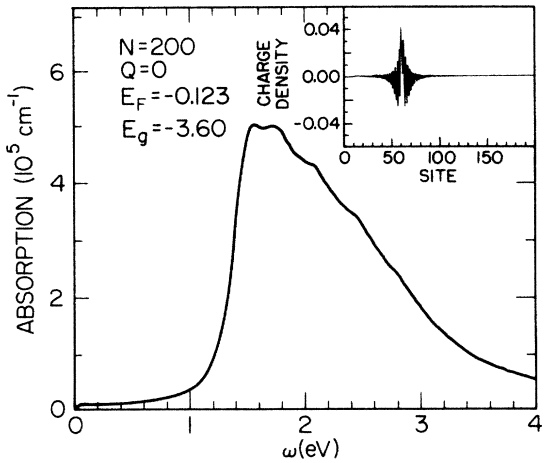


FIG. 1. Optical absorption as a function of frequency and charge distribution in units of electron charge for neutral-dimerized *trans*-polyacetylene chains with 200 CH groups and an impurity adjacent to site 61. $E_F$ is the Fermi energy relative to the middle of the energy gap and $E_g$ is the ground-state energy of the chain relative to the uniform chain with the same $N$.

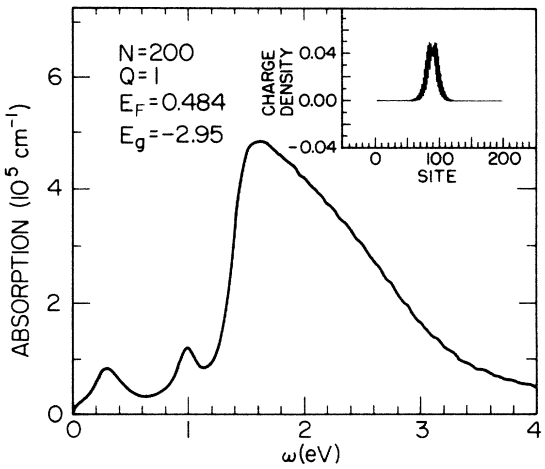


FIG. 2. Optical absorption and charge distribution for charged *trans*-polyacetylene chains with 200 CH groups and a polaron centered at site 90. There are no impurities near the chain.

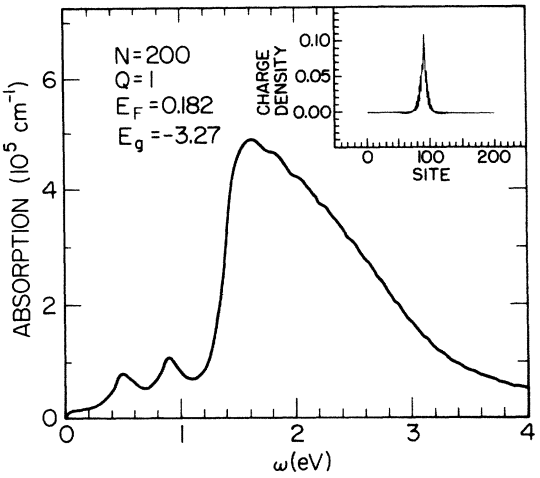


FIG. 3. Optical absorption and charge distribution for charged *trans*-polyacetylene chains with 200 CH groups. A polaron is centered at site 90, adjacent to an impurity.

whereas the charged-polaron spectra show a minimum there. Thus, it is unlikely that polarons play a major role in determining the spectrum.

The spectrum has been taken as evidence for the presence of solitons in *trans*-polyacetylene. Solitons (or kinks) are lattice distortions which change the dimerization symmetry from strong-weak to weak-strong (or vice versa) on successive odd-even sites along the chain. The change is accomplished gradually using the SSH form:

$$u_n=(-1)^n u_0 \tanh[(n-k)/l] \tag{10}$$

for a soliton of width $l$ centered at site $k$. The soliton is energetically favored on a chain with an odd number of CH sites since it allows both ends of the chain to have strong bonds. A weak-end bond costs 1.07 eV more in energy than a strong-end bond, and more than compensates the 0.44 eV needed for creating a soliton on the chain. The properties of free solitons have been well studied. When no impurities are present, a chain with a soliton has a localized single-particle energy level at the middle of the gap between the valence band and the conduction band. This state is called the soliton state and it gives rise to an optical-absorption spectrum that exhibits a peak which onsets at the middle of the BI region.[1] Figure 4 shows how the peak appears when lifetime broadening is taken into account. The peak is due to transitions into or out of the mid-gap state and, due to charge-conjugation symmetry, the spectrum is the same whether the chain is charged or not. When the chain is neutral and there are no impurities near the chain, charge is distributed uniformly on the lattice sites just as for the pure-dimerized cases. Changes occur in the valence-band states due to the kink distortion, and they compensate for the creation of the mid-gap state. The charge distribution shown in the insert of Fig. 4 for the charged chain has the form expected for an extra electron in the soliton state.[7]

Whereas for pristine *trans*-polyacetylene (no impurities) the spectrum is the same for the charged and uncharged chain and there is no energy gap for adding or taking an electron off the chain, the situation changes in the presence of an impurity. We will consider three cases: (i) the impurity adjacent to a site well within the chain and a soliton bound to the impurity; (ii) the impurity near the end of the chain and a soliton centered near the impurity; and (iii) the impurity near the end of the chain and a free soliton well within the chain.

The optimum soliton width for a kink bound to an impurity has been shown[6,13] to be $l=4$ or 5. We used $l=5$ for the results reported here. Figure 5 is for a chain of $N=199$ CH groups with an impurity adjacent to a site

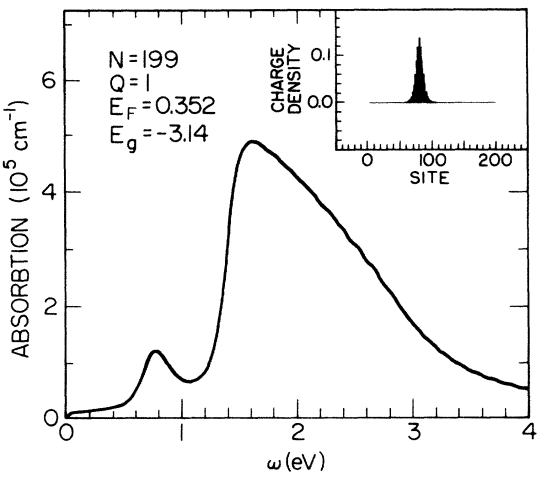


FIG. 4. Optical absorption and charge distribution for charged *trans*-polyacetylene chains with 199 CH groups and a soliton centered at site 80. There are no impurities near the chain.

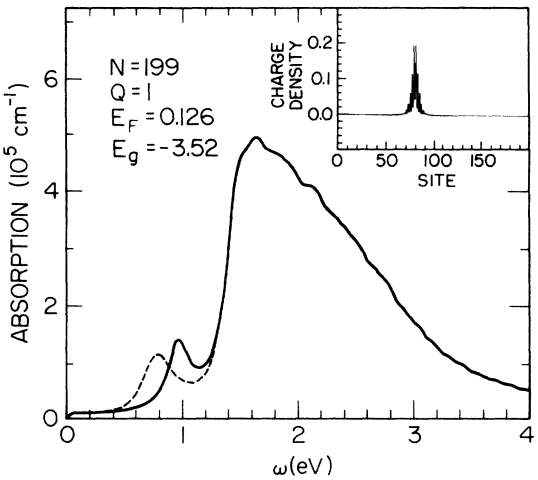


FIG. 5. Optical absorption and charge distribution for *trans*-polyacetylene chains with 199 CH groups. An impurity is adjacent to site 80, and a soliton is centered at the impurity. The dashed line shows the optical absorption in the absence of the impurity (see Fig. 4).

well within the chain and a kink centered at the same site. In the presence of the impurity, charge collects around the impurity site to screen it. If the chain is neutral, the charge oscillates in sign outside of the immediate region of the soliton. If the chain picks up charge, the charge concentrates over about ten lattice sites on either side of the impurity. The optical-absorption spectrum of the neutral chain exhibits a shoulder in addition to a peak. The shoulder is due to transitions from the valence band into the half-filled soliton state, with a threshold at 0.38 eV for the impurity described in Sec. II. In the more-likely case when the chain is charged, the soliton state is full and the shoulder disappears. The peak is stronger as there are now two electrons which can be excited from the soliton level at $-0.347$ eV to an impurity level at 0.600 eV. Note, however, this peak is no longer at mid-gap. Its threshold is at 0.947 eV which is considerably above the threshold suggested by experimental observations[1-4] in $(CH)_x$, and it is narrower than the free-soliton peak shown for comparison by the dashed line in Fig. 5.

If the impurity is at the end of the chain with the soliton "centered" at the end [i.e., $k=0$, $l=5$ in Eq. (10)] one obtains the optical-absorption spectrum shown in Fig. 6. The spectrum does not show much BI absorption, and there is no trace of the characteristic soliton "mid-gap" peak. Note, however, that it is energetically more favorable for a soliton to be bound to an impurity well within a chain than at the end of a chain, the energy difference being 0.28 eV for a charged chain.

Finally we consider the case where the impurity is at the end of the chain but the soliton is a free soliton, well within the chain. The spectrum, Fig. 7, shows the characteristic mid-gap soliton peak whether or not the chain is charged. The ground-state energy of the charged chain is only 0.05 eV higher than for a soliton bound to an end impurity. It is known that solitons are repelled by chain ends. Su[14] found the repulsion to be approximately 0.28 eV for a free soliton (see his Fig. 3) on a semi-infinite

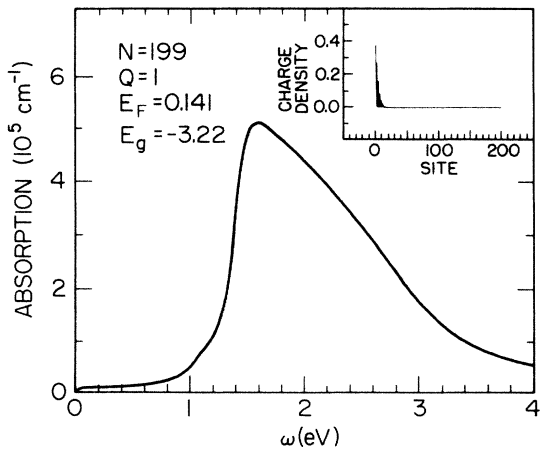


FIG. 6. Optical absorption and charge distribution for *trans*-polyacetylene chains with 199 CH groups. An impurity is near the end (site 1) and a soliton is "centered" at the impurity.

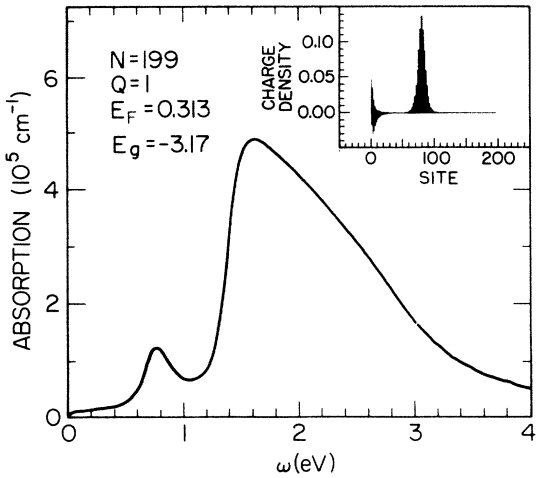


FIG. 7. Optical absorption and charge distribution for *trans*-polyacetylene chains with 199 CH groups. An impurity is near the end (site 1) and a "free" soliton is centered at site 80.

chain with 49 additional sites. We find 0.31 eV for this energy of repulsion calculated for finite chains with $N=199$ or $N=200$. This energy reflects loss of one-half of the lattice-energy lowering associated with the gradual change of dimerization when the kink is at an end. Using these results, we can roughly understand the energy found for a chain with end impurity. When an impurity is at the end of the chain, the charged soliton is attracted to the impurity by approximately the same binding energy as at an interior site (0.35 eV), but repelled from the chain end by 0.31 eV, leaving the bound-soliton case lower as noted above. Overall, the charged soliton bound to the end impurity is more favorable, but the binding energy is so small that thermal fluctuations may be able to free the soliton. Once freed, the charge on the soliton is only weakly bound to the chain and it could become available for interchain conduction. When the soliton is uncharged, it is only weakly attracted to the impurity. Thus, the end repulsion dominates and the free soliton is favored.

The configuration with the impurity at the end of the chain is higher in energy than if the impurity were within the chain; nevertheless, the optical-absorption spectrum and low binding energy of the additional charge are both features that are consistent with the observed properties of doped $(CH)_x$. This suggests that the doping process may proceed so as to favor impurity-ended chains, or lead to structures that simulate their effect. We will return to this question in Sec. IV.

For our calculations of the conductivity, Eq. (5), we used a lifetime parameter $\eta=0.1$ eV. Increasing $\eta$ reduces the mid-gap and interband peaks and broadens them. The effect of changing $\eta$ is shown in Fig. 8 for a pure chain with $N=99$ sites. Keeping $\eta$ finite provides a way to account for the averaging over different numbers of ions on a chain and also for some higher-order many-body effects. The bulk of the results reported in this paper were for $N\sim200$, corresponding to an impurity concentration of 0.5% In actual films a range of $N$ is to be expected.

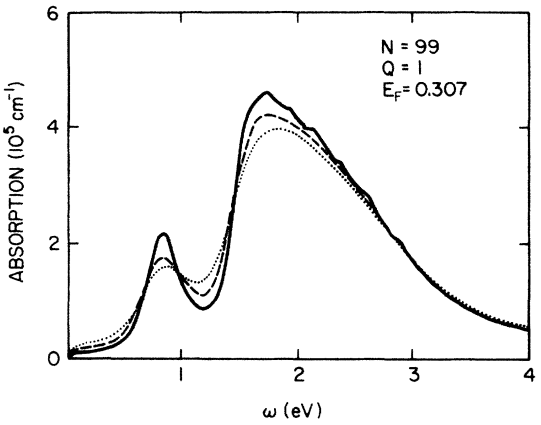


FIG. 8. The effect of the lifetime parameter $\eta$ on the optical absorption spectrum of a polyacetylene chain with 99 sites. Solid line: $\eta=0.1$; dashed line: $\eta=0.15$; dotted line: $\eta=0.2$.

## IV. DISCUSSION

Comparison of our results for optical absorption with the experimental spectra observed for films of *trans*-polyacetylene gives insight into the microstructure of the films. For pristine polyacetylene there is a notable absence of absorption below the interband threshold,[1-4] indicating the absence of chains with an odd number of CH units. As we have seen, odd chains show a peak near mid-gap due to the energetically favored configuration with a soliton within the chain and strong-end bonds. Even chains may be initially favored in the preparation of polyacetylene films insofar as the chains are formed by the accreting of acetylene molecules, each of which adds two carbon atoms to the chain. In addition, comparing ground-state energies of the neutral system shows that even chains are intrinsically more stable than odd chains because of the energy needed to form the free soliton.

The situation is altered when impurities are introduced into the film, and the chains are charged. The optimum configuration in this case is the odd-sited chain with a soliton bound to the impurity (Fig. 5). However, the optical-absorption spectrum with a bound soliton has a BI peak near $\hbar\omega=1$ eV which is considerably above the 0.7 eV onset of the experimental spectrum. Feldblum *et al.*[3] have suggested that the discrepancy would be removed if electron-electron interactions were taken into account. The effect of electron-electron interactions is still under investigation.[22-25] Results, other than for spin density, tend to support the qualitative conclusions of the one-electron theory. However, to our knowledge, there are no results reported to date for the combined effects of impurities and interactions. Interchain coupling has also been neglected in our treatment. It is known to affect soliton confinement[26,27] and could also alter the chain-energy assignments we have found. In any case, the differences between the observed and calculated onset energy and width of the BI absorption are evidence of the inadequacy of the model which treats polyacetylene as composed of infinitely long chains governed by the SSH Hamiltonian.

Consideration of electrical conductivity also poses a problem for the theory. The conductivity of polyacetylene films increases by many orders of magnitude due to doping.[28] The conductivity increase has been considered to be associated with the introduction of solitons. Free solitons are highly mobile on $(CH)_x$ chains. However, in the presence of impurities the solitons are bound and a more elaborate explanation is required. Kivelson[29] proposed that the conductivity results from a charge-exchange process between free and bound solitons. The origin of the additional free solitons remains to be explained.

Our results indicate a possible mechanism for the introduction of free solitons. Solitons will be introduced if the doping process causes an effective breaking of chains. While it is unlikely that an off-chain impurity will actually sever a strong $\sigma$ bond, it may distort the chain and make $\pi$ bonding between the carbon sites very unfavorable. Then the neighborhood of the impurity could act as a chain end for the $\pi$-electron states. "Breaks" could occur at strong or weak bonds. Breaking a weak bond results in two even chains with strong-end bonds. Breaking a strong bond results in two chains with $N$ odd and each having one weak-end bond. Since a weak-end bond is so energetically unfavorable, a soliton will be generated at the end and can migrate into the chain as in Fig. 9(a). A neutral soliton will migrate in due to end repulsion. A charged soliton may remain at the end due to pinning to the impurity which caused the break. However, as discussed in Sec. III, the pinning of a charged soliton to an impurity at the end of a chain is weak, and thermal fluctuations may free it. Once freed, the charge on the soliton has little Coulomb binding to the chain and is available for interchain-hopping conduction.

This scenario indicates how doping can give rise to free rather than pinned soliton behavior. There still are unanswered questions associated with this description, the most immediate being the question of how the impurities affect the lattice. Chien[30] has proposed several chain-impurity configurations in which the impurity is chemically bound to the chain. Further study is needed to clarify their effect on chain wave functions and energy levels. If $\pi$-electron states near the gap edges are effectively isolated to one or the other side of the impurity complex, then the result may be similar to actual chain breaking, and may have a similar effect for soliton creation and pinning. Gibson *et al.*[31] have reported evidence of remnant cis-linkage in *trans*-polyacetylene and suggested that linkages limit soliton motion and give short effective chain lengths. Charged impurities could cause chains to deform or favor cis-type linkages with a similar effect on soliton mobility. However, to our knowledge, detailed analyses of these configurations are not yet available.

For even $N$ we expect polaron distortions to occur on charged chains; however, as discussed in Sec. III, the observed absorption spectrum shows no evidence of polaron contributions. Onodera and Okuno have studied two mechanisms which could contribute to the disappearance of polarons on a $(CH)_x$ chain.[32,33] The first mechanism is the meeting of two charged polarons which then decay

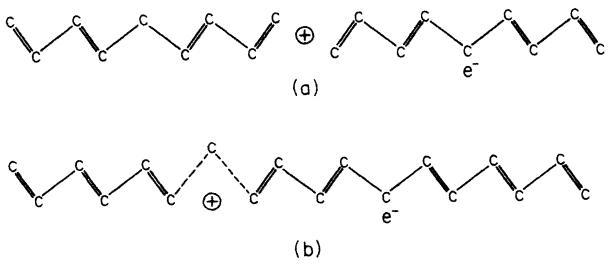


FIG. 9. Possible effects of an impurity atom on a polyacetylene chain. (a) The impurity separates the chain into two segments. If the resulting segments have odd $N$, then solitons form to preserve strong-end bonds. (b) The impurity causes the displacement of a carbon atom off the chain axis, effectively breaking the chain into an odd-$N$ and an even-$N$ segment. A soliton forms on the odd segment to preserve strong-end bonds.

into two charged solitons.[32] However, such a process is unlikely if the polarons are pinned to different impurities. Comparison of the ground-state energies in Figs. 2 and 3 shows that the pinning energy is 0.34 eV. The second mechanism is the interaction of a neutral soliton and a charged polaron to form a charged soliton plus radiation.[33] Both of these reactions require the spins of the initial defects to be antiparallel, and the latter one still requires a source for the additional neutral solitons. An additional way for polarons to disappear is through charge fluctuation. If the chain is neutralized by charge leaving the partially filled polaron state, then the polaron becomes unstable to collapse into the neutral-dimerized lattice, which has lower energy. The extra charge can carry off up to 0.33 eV to help it overcome or tunnel through the interchain barrier and reach an odd-sited chain with an unfilled soliton state. There is evidence for the presence of polarons in photogenerated optical absorption.[34] By studying the time evolution of the photogenerated-absorption spectrum it should be possible to determine the polaron lifetime on a chain.

The effect of compensation on doped polyacetylene has posed a problem for the soliton theory.[35] Compensated samples show reduced conductivity and a disappearance of mid-gap optical absorption. If mid-gap absorption and impurity-induced conductivity are a consequence of soliton creation, then it is not obvious from the usual description why they disappear when the samples are compensated by further doping by oppositely charged impurities. Charge-conjugation invariance suggests that additional oppositely charged solitons would be created. In order to annihilate, oppositely charged solitons must be on the same chain and be able to overcome pinning potentials. A possible clue to the effect of compensation lies in the pseudo-chain-breaking picture which we have proposed. It is possible that the compensation process "relinks" broken bonds as the original impurities are neutralized. Bond breaking and relinking need not involve large-scale displacements of lattice ions. Figure 9(b) suggests how an impurity might cause the displacement of a carbon atom away from a $(CH)_x$ chain and effectively break it into two segments, one even and one odd. Neutralizing the impurity would allow the chain to regain its original configuration. Further study is clearly needed to work out the details of the doping and compensation processes.

Finally, we want to discuss the relationship between the optical-absorption spectra we have found, and that measured experimentally. Real films are a complex of many chains. A range of $N$ is to be expected and there may be a variety of chain configurations present. There can be neutral purely dimerized segments with even-$N$, and odd-$N$ segments with kink distortions. Also the impurities may lie at varying distances from the chain. Actual films are usually anisotropic with chains at different orientations relative to the film surface.[36] The spectrum would then be a composite of all these effects. If samples can be prepared which control these factors, then it should be possible to analyze the composition by comparison with the single-chain spectra presented in this paper.

## ACKNOWLEDGMENTS

Computer time for this project was supplied by the Computer Science Center of the University of Maryland. We would also like to thank Dr. C. Hicks for useful discussions, and Dr. C. S. Wang for help with the computer calculations. A longer unpublished version of the present paper (Ref. 11) was prepared while one of us (A.J.G.) was a guest of Tel Aviv University.

[1]N. Suzuki, M. Ozaki, S. Etemad, A. J. Heeger, and A. G. MacDiarmid, Phys. Rev. Lett. **45**, 1209 (1980).
[2]H. Kiess, W. Meyer, D. Baeriswy, and G. Harbeke, J. Electron. Mater. **9**, 763 (1980).
[3]A. Feldblum, J. H. Kaufman, S. Etemad, A. J. Heeger, T.-C. Chang, and A. G. MacDiarmid, Phys. Rev. B **26**, 815 (1982).
[4]M. Tanaka, A. Watanabe, and J. Tanaka, Bull. Chem. Soc. Jpn. **53**, 645 (1980); **53**, 3430 (1980).
[5]M. J. Rice, Phys. Lett. **71A**, 152 (1979).
[6]W. P. Su, J. R. Schrieffer, and A. J. Heeger, Phys. Rev. Lett. **42**, 1698 (1979).
[7]W. P. Su, J. R. Schrieffer, and A. J. Heeger, Phys. Rev. B **22**, 2099 (1980).
[8]S. Kivelson, T.-K. Lee, Y. R. Lin Liu, I. Peschel, and Lu Yu, Phys. Rev. B **25**, 4173 (1982).
[9]J. C. Hicks and A. L. Wasserman, Phys. Rev. B **29**, 808 (1984).
[10]B. Horowitz, Solid State Commun. **41**, 593 (1982).
[11]A. J. Glick and G. W. Bryant, Tel Aviv University Report No. TAUP-1368-85, 1985 (unpublished).
[12]G. W. Bryant and A. J. Glick, J. Phys. C **15**, L391 (1982).
[13]G. W. Bryant and A. J. Glick, Phys. Rev. B **26**, 5855 (1982).
[14]W. P. Su, Solid State Commun. **35**, 899 (1980).
[15]D. Vanderbilt and E. J. Mele, Phys. Rev. B **22**, 3939 (1980).
[16]S. Stafström and K. A. Chao, Phys. B **29**, 2010 (1984).
[17]A. J. Glick and G. W. Bryant, University of Maryland Technical Report PP 82-047, 1982 (unpublished).
[18]A. J. Glick, Phys. Rev. Lett. **49**, 804 (1982).
[19]S. A. Brazovskii and N. N. Kirova, Pis'ma Zh. Eksp. Teor. Fiz. **33**, 6 (1981) [JETP Lett. **33**, 4 (1981)].
[20]D. K. Campbell and A. R. Bishop, Phys. Rev. B **24**, 4859 (1981).
[21]J. P. Albert and C. Jouanin, Solid State Commun. **47**, 825

(1983).
[22]J. E. Hirsch and M. Grabowski, Phys. Rev. Lett. **52**, 1713 (1984).
[23]See e.g., D. K. Campbell, T. A. DeGrand, and S. Mazumdar, Phys. Rev. Lett. **52**, 1717 (1984), and references therein.
[24]Z. G. Soos and S. Ramasesha, Phys. Rev. B **29**, 5410 (1984).
[25]V. Mujica, N. Castor, and O. Goscinski, Phys. Rev. B **32**, 4178 (1985); **32**, 4186 (1985).
[26]D. Baeriswyl and K. Maki, Phys. Rev. B **28**, 2068 (1983).
[27]R. H. Baughman and G. Moss, J. Chem. Phys. **77**, 6321 (1982).
[28]C. K. Chiang, C. R. Fincher, Jr., Y. W. Park, and A. J. Heeger, Phys. Rev. Lett. **39**, 1098 (1977).
[29]S. Kivelson, Phys. Rev. Lett. **46**, 1344 (1981); Phys. Rev. B **25**, 3798 (1982).
[30]J. C. W. Chien, J. Polym. Sci., Polym. Lett. Ed. **19**, 249 (1981).
[31]H. W. Gibson, R. J. Weagley, R. A. Mosher, S. Kaplun, W. M. Prest, Jr., and A. J. Epstein, Phys. Rev. B **31**, 2338 (1985).
[32]Y. Onodera and S. Okuno, J. Phys. Soc. Jpn. **52**, 2478 (1983).
[33]S. Okuno and Y. Onodera, J. Phys. Soc. Jpn. **52**, 3495 (1983).
[34]J. Orenstein, Z. Vardeny, G. L. Baker, G. Eagle, and S. Etemad, Phys. Rev. B **30**, 786 (1984).
[35]B. R. Weinberger, C. B. Roxlo, S. Etemad, G. L. Baker, and J. Orenstein, Phys. Rev. Lett. **53**, 86 (1984).
[36]A. J. Glick and G. W. Bryant, Phys. Rev. B **28**, 4295 (1983).